

Review

Cr₇Ni Wheels: Supramolecular Tectons for the Physical Implementation of Quantum Information Processing

Jesus Ferrando-Soria [†]

School of Chemistry, University of Manchester, Oxford Road, Manchester M13 9PL, UK; jesus.ferrando@uv.es;
Tel.: +34-963-544460

[†] Present address: Instituto de Ciencia Molecular (ICMol), Universitat de València, Paterna 46980, València, Spain.

Academic Editor: Floriana Tuna

Received: 11 August 2016; Accepted: 15 September 2016; Published: 21 September 2016

Abstract: The physical implementation of quantum information processing (QIP) is an emerging field that requires finding a suitable candidate as a quantum bit (qubit), the basic unit for quantum information, which can be organised in a scalable manner to implement quantum gates (QGs) capable of performing computational tasks. Supramolecular chemistry offers a wide range of chemical tools to bring together, with great control, different molecular building blocks in order to grow supramolecular assemblies that have the potential to achieve the current milestones in the field. In this review, we are particularly interested in the latest research developments on the supramolecular chemistry approach to QIP using {Cr₇Ni} wheels as qubits for the physical implementation of QGs. Special emphasis will be given to the unique high degree of chemical tunability of this unique class of heterobimetallic octanuclear rings, which results in an attractive playground to generate aesthetically pleasing supramolecular assemblies of increasing structural complexity and interesting physical properties for quantum computing.

Keywords: {Cr₇Ni} heterobimetallic rings; quantum information processing; supramolecular chemistry; qubits; quantum gates

1. Introduction: Molecules as Qubits

The physical implementation of quantum information processing (QIP) is currently a subject of intense research in chemistry, physics, materials science, and nanotechnology because of the thrilling potential technological applications that chemical and physical systems may exhibit in quantum computing [1–4]. QIP offers the possibility to outperform conventional computers in some computational tasks, such as searching unsorted directories and factoring large numbers in primes [5,6]. However, a major challenge in developing devices for quantum computation relies on finding suitable candidates for use as quantum bits (qubits), the basic units used for quantum information, which can be brought together in an organised, scalable, and addressable way to build quantum gates (QGs) capable of performing useful logic algorithms [3,4].

Magnetic molecules [7–24] could present some disadvantages in comparison with other quantum systems for QIP. For example, as individual units, molecular electron spin-based qubits may not have such long phase memory times [25–29]. However, we could take advantage of the two-fold degree of the chemical tunability of molecules, at the molecular and supramolecular levels, to improve their performance as qubits. At the molecular level, this has been well demonstrated in the last few years by the careful chemical design of tailor-made molecules, where the number of protons and other atoms with a nuclear magnetic moment have been minimised in order to increase the phase memory times [14,18,21,22]. This has been recently extended to the chemical design of molecules with crystal field ground states possessing large tunneling gaps that give rise to atomic clock transitions,

at which the quantum spin dynamics become protected against dipolar decoherence [24]. Yet the main advantage of molecular qubits resides in their further chemical engineerability at the supramolecular level. The potential applicability of supramolecular chemistry [30–34] make molecules unique quantum systems where we could precisely tune the intermolecular interaction between qubits in terms of their spatial orientation, strength, and homo-/heterogeneous nature. Thus, this represents a key feature to be exploited by chemistry, in order to build supramolecular arrays of molecular qubits in a controlled manner, which could efficiently implement multiple qubit-based QGs.

During the last few years, a large effort has been put forth by several research groups worldwide with the intention of increasing the phase memory times of molecular qubits. Several quantum systems that have been proposed as qubits exhibit excellent performance as individual sites, such as ^{13}C sites near nitrogen vacancies in diamond, but often such qubits are difficult to link controllably into useful arrays [27]. In a pioneering work, Leuenberger and Loss proposed the use of molecular nanomagnets, such as $[\text{Mn}_{12}\text{O}_{12}(\text{O}_2\text{CCH}_3)_{16}(\text{H}_2\text{O})_4]$, abbreviated as $[\text{Mn}_{12}]$ [7], as electron spin-based qubits. Since then, a wide range of magnetic molecules have been synthesised, either small mono- and dinuclear complexes or large polynuclear clusters with transition metals and lanthanide ions [12,14–24]. A measure of the quality of a qubit against decoherence processes is provided by the spin-spin relaxation time (T_2) and the phase memory time (T_M), measured through pulsed EPR spectroscopy [35]. Strictly speaking T_2 and T_M are not the same, but frequently in the literature they are used indistinctly. In fact, T_M is a generic term that encompasses all processes that cause the loss of electron spin phase coherence. T_2 is just one of the contributors. Only in the case where the phase memory decay function is a monoexponential can both parameters be considered as equivalents. In this respect, the latest results obtained with square planar copper(II)-phthalocyaninato and bis(maleonitriledithiolato), $[\text{Cu}(\text{pc})]$ and $(\text{Ph}_4\text{P})_2[\text{Cu}(\text{mnt})_2]$ are remarkable [16,18]. T_2 values in the range of 2.6 μs to 1.0 μs at 5 and 80 K, just above the boiling temperatures of liquid He and N_2 , respectively, have been reached for a diluted thin-film of the $[\text{Cu}(\text{pc})]$, while T_M values of about 0.6 μs at room temperature have been observed for a doped matrix of $(\text{Ph}_4\text{P})_2[\text{Cu}(\text{mnt})_2]$. Additionally, the latest results obtained with octahedral vanadium(IV)-tris(2,5-dithioxobenzol[1,2-d:3,4-d']bis[1,3]dithiolene-7,8-dithiolato), $(\text{Ph}_4\text{P})_2[\text{V}(\text{dbmit})_3]$, and square pyramidal vanadyl(IV)-phthalocyanine, $[\text{VO}(\text{pc})]$, with T_M values up to 700 μs at 10 K and 0.8 μs at 300 K, respectively, clearly reflect the progress being made in the field [21,22].

Among the different molecular qubit approaches proposed in the literature, this review focuses on the studies of $\{\text{Cr}_7\text{Ni}\}$ wheels performed by Winpenny's group in Manchester, UK, where this two-fold degree of chemical engineering has been conveniently exploited, first with single wheels at the molecular level, and then at the supramolecular level to obtain dimeric and eventually oligomeric wheel assemblies.

2. Individual $\{\text{Cr}_7\text{Ni}\}$ Wheels as Single Qubits

$\{\text{Cr}_7\text{Ni}\}$ wheels consist of anionic fluoridebis(carboxylate)-bridged octanuclear chromium(III)-nickel(II) complexes with ring topology of the general formula $\text{A}[\text{Cr}_7\text{NiF}_8\text{L}_{16}]$, where L could be diverse carboxylate bridging ligands such as acetate (ac), trichloroacetate (tcac), propionate (prop), pivalate (piv), 1-methylcyclohexanecarboxylate (mcyca), 1-adamantylcarboxylate (adca), 3-thiophenecarboxylate (thca), benzoate (bz), or pentafluorobenzoate (pfbz), and A^+ is a central templating cation, either organic or inorganic such as R_2NH_2^+ ($\text{R} = \text{Me}, \text{Et}, \text{and Pr}$) or Cs^+ (Figure 1) [36–38]. These $\{\text{Cr}_7\text{Ni}\}$ wheels were prepared by adapting the method previously reported for the parent neutral octanuclear homometallic chromium(III) wheels of formula $[\text{Cr}_8\text{F}_8\text{L}_{16}]$, abbreviated as $\{\text{Cr}_8\}$, by replacing one Cr^{III} ion with a Ni^{II} ion through the aid of a counterbalancing dialkylammonium, such as Pr_2NH_2^+ , which simultaneously acts as templating agent [38]. In contrast to the parent antiferromagnetically coupled $\{\text{Cr}_8\}$ wheels, which possess a diamagnetic ground state ($S = 0$), these $\{\text{Cr}_7\text{Ni}\}$ wheels exhibit a $S = 1/2$ ground state resulting from the non-compensation of the intramolecular antiferromagnetic coupling between the seven Cr^{III} ions ($S_{\text{Cr}} = 3/2$) and the single high-spin Ni^{II} ion ($S_{\text{Ni}} = 1$).

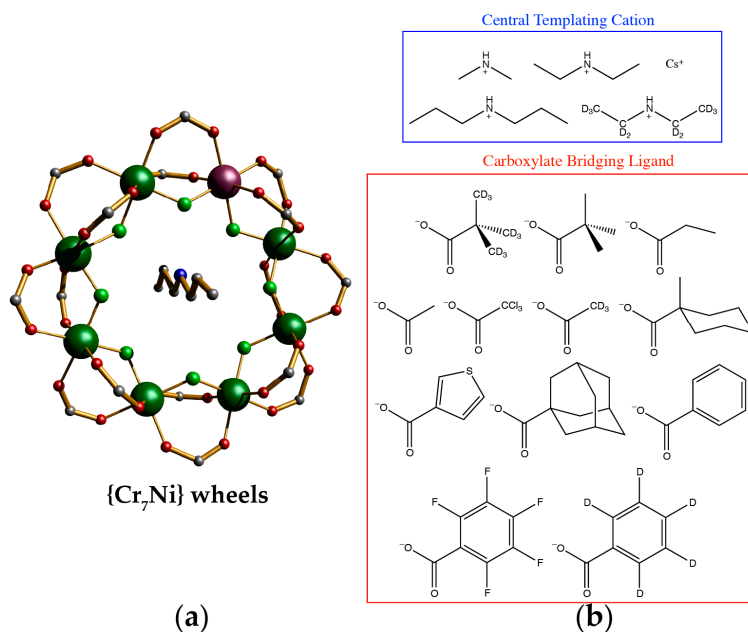


Figure 1. (a) Crystal structure of {Cr₇Ni} wheels, shown with Pr₂NH₂ as the templating cation. Colour code: Cr, green; Ni, purple; N, blue; O, red; C, grey; F, pale green. H atoms and tertiary butyl groups from the carboxylate bridging ligand are omitted for clarity (reproduced with permission from (C. J. Wedge et al.), (Physical Review Letters); published by (American Physical Society), (2012)); (b) Chemical structures of some possible variants of both the central templating cation and the carboxylate bridging ligand of {Cr₇Ni} wheels (blue and red boxes, respectively).

Winpenney has proposed using {Cr₇Ni} wheels as a molecular qubit for QIP [9]. In fact, the $S = 1/2$ ground state of {Cr₇Ni} wheels is a two-level quantum system (0 and 1 of the qubit are then $m_S = +1/2$ and $m_S = -1/2$ levels, respectively) which meets the criteria required for qubits, e.g., it is possible to initialise them and the scale of energies is appropriate [9]. {Cr₇Ni} wheels have sufficient T_M values to allow gate operation before state degradation can occur [14], and thus it is possible to have control of the interaction between the entangled states [39].

Besides their high chemical stability in solution, the most striking feature is the vast chemical versatility that {Cr₇Ni} wheels possess at the molecular level. This has allowed for the synthesis of a plethora of wheels with different templating cations and carboxylate bridging ligands, which make them an extraordinary platform to study the influence of the nature of different components on their phase memory times, through pulsed EPR spectroscopic measurements in toluene [38].

For instance, the variation of the dialkylammonium cation and the carboxylate ligand allows for the modification of the values of T_M at 5 K following the trend 0.38 (Me₂NH₂⁺) < 0.62 (Pr₂NH₂⁺) < 0.73 μs (Et₂NH₂⁺) and 0.34 (prop) < 0.44 (ac) < 0.62 μs (piv) along the two related series of the general formula R₂NH₂[Cr₇NiF₈(piv)₁₆] and Pr₂NH₂[Cr₇NiF₈L₁₆], respectively (Table 1) [14]. Moreover, the T_M value can be further optimised to 0.93 μs at 5 K after complete deuteration of the pivalate ligand and/or the Et₂NH₂⁺ cation for the {Cr₇Ni} wheels with dialkylammonium cations, while T_M values up to 15.3 μs at 1.5 K have been reached for the {Cr₇Ni} wheels with Cs⁺ as a templating cation and perdeuterated pivalate in deuterated toluene (Table 1).

Kaminski et al. have further attempted to investigate the effect of replacing hydrogen atoms with deuterium and halogens, such as fluorine and chlorine, at the acetate and benzoate bridging ligands, respectively, on the quantum coherence properties of the corresponding Cr₇Ni wheels, both in toluene and deuterated toluene solutions [40]. For instance, the values of T_M at 5 K along the series of {Cr₇Ni} wheels of general formula Pr₂NH₂[Cr₇NiF₈L₁₆] follow the trend 0.4 (tfbz) < 0.9 (d-bz) < 1.0 μs (bz) in deuterated toluene (Table 1).

Overall, the unique chemical flexibility of {Cr₇Ni} wheels at the molecular level have allowed us to obtain control of the phase memory time, as well as to identify the coupling between electron and nuclear spins for these types of molecular nanomagnets as the main source of decoherence, even if other sources of decoherence ligated to molecular motions (spectral diffusion) cannot be totally neglected.

Table 1. Selected phase memory times for different {Cr₇Ni} wheels.

Compound ^a	T/K	T _M ^b /μs
Me ₂ NH ₂ [Cr ^{III} ₇ Ni ^{II} F ₈ (piv) ₁₆] ^c	5.0	0.38
	1.8	0.55
<i>d</i> -Me ₂ NH ₂ [Cr ^{III} ₇ Ni ^{II} F ₈ (<i>d</i> -piv) ₁₆] ^c	1.8	3.8
Et ₂ NH ₂ [Cr ^{III} ₇ Ni ^{II} F ₈ (piv) ₁₆] ^c	5.0	0.73
Et ₂ NH ₂ [Cr ^{III} ₇ Ni ^{II} F ₈ (<i>d</i> -piv) ₁₆] ^c	5.0	0.93
<i>d</i> -Et ₂ NH ₂ [Cr ^{III} ₇ Ni ^{II} F ₈ (<i>d</i> -piv) ₁₆] ^c	5.0	0.93
Pr ₂ NH ₂ [Cr ^{III} ₇ Ni ^{II} F ₈ (piv) ₁₆] ^c	5.0	0.62
Cs[Cr ^{III} ₇ Ni ^{II} F ₈ (piv) ₁₆] ^c	5.0	0.74
Cs[Cr ^{III} ₇ Ni ^{II} F ₈ (<i>d</i> -piv) ₁₆] ^c	5.0	0.89
Cs[Cr ^{III} ₇ Ni ^{II} F ₈ (<i>d</i> -piv) ₁₆] ^d	5.0	15.3
Pr ₂ NH ₂ [Cr ^{III} ₇ Ni ^{II} F ₈ (prop) ₁₆] ^c	5.0	0.34
Pr ₂ NH ₂ [Cr ^{III} ₇ Ni ^{II} F ₈ (ac) ₁₆] ^c	5.0	0.44
Pr ₂ NH ₂ [Cr ^{III} ₇ Ni ^{II} F ₈ (bz) ₁₆] ^d	5.0	1.0
Pr ₂ NH ₂ [Cr ^{III} ₇ Ni ^{II} F ₈ (<i>d</i> -bz) ₁₆] ^d	5.0	0.90
Pr ₂ NH ₂ [Cr ^{III} ₇ Ni ^{II} F ₈ (pfbz) ₁₆] ^d	5.0	0.40

^a Ligand abbreviations: ac = acetate; prop = propionate; piv = pivalate; *d*-piv = deuterated pivalate; bz = benzoate; *d*-bz = perdeuterated benzoate; pfbz = pentafluorobenzoate (see Figure 1); ^b Value of the phase memory time determined through pulsed EPR spectroscopic measurements; ^c In a 0.1 mM solution of toluene; ^d In a 0.1 mM solution of deuterated toluene.

3. Dimeric Assemblies of {Cr₇Ni} Wheels as Double Qubit-Based Quantum Gates

In addition to the quantum coherence properties of molecular qubits, another key parameter for QIP is the timescale to perform a two-qubit gate. This time is inversely proportional to the strength of the interaction between the individual qubits. Performing quantum computation is then vital to possess a precise control of the inter-qubit interaction. This has to be strong enough to obtain a gate time shorter than the phase memory time of qubits, otherwise the information will be lost through decoherence. However, it cannot be too strong, otherwise the gate time would be shorter than the time needed to manipulate a single spin—in pulsed EPR spectroscopy this time is around 10 ns [41].

A close analysis of the chemical structure of {Cr₇Ni} wheels clearly reveal three possible synthetic routes to functionalise single wheels at the molecular level in order to link them together into a supramolecular dimeric assembly, which could eventually give rise to a two-qubit quantum gate. The first route would involve the creation of an accessible metal site with which a bis(monodentate) bridging ligand could coordinate. The second route would require functionalisation within the carboxylate ligands that allow {Cr₇Ni} wheels to act as metalloligands towards other metal complexes acting in turn as central linkers. Finally, the third route would involve the synthesis of more complex templating ammonium cations acting as the threads of {Cr₇Ni} wheels in the resulting rotaxanes.

3.1. {Cr₇Ni} Wheels with Open Metal Sites as Metal Complexes

The first avenue consists of replacing some of the bridging fluoride by adding *N*-ethyl-*D*-glucamine (H₅Etglu) as an additional proligand to the reaction between hydrated chromium(III) fluoride and a nickel(II) source in pivalic acid. The resulting wheel has the formula [Cr₇NiF₃(Etglu)(O₂C^{*t*}Bu)₁₅(H₂O)], abbreviated as {Cr₇Ni}' , where the polyalcohol proligand is completely deprotonated and the five alkoxide groups replace five fluoride anions [42]. The most striking feature of this {Cr₇Ni}' wheel is the presence of a labile terminal water molecule bound to the nickel(II) site, which can be easily displaced by reaction with oligopyridines or related polyazines and

polyazoles [41–45]. For instance, Bellini et al. have prepared a series of wheel dimers of the general formula $[\{Cr_7NiF_3(Etglu)(piv)_{15}\}_2L]$ [L = pyrazine (pyr), bis(dimethylpyrazolyl) (bpz), 4,4'-bipyridine (4,4'-bpy), *trans*-bipyridylethene (bpe), and bipyridylbenzene (bpbz)], abbreviated as $\{Cr_7Ni\}'_2L$, as depicted in Figure 2. In particular, the dimer of formula $[\{Cr_7NiF_3(Etglu)(piv)_{15}\}_2(4,4'\text{-bpy})]$ constitutes the first example of the rational design of entangled double qubits [44].

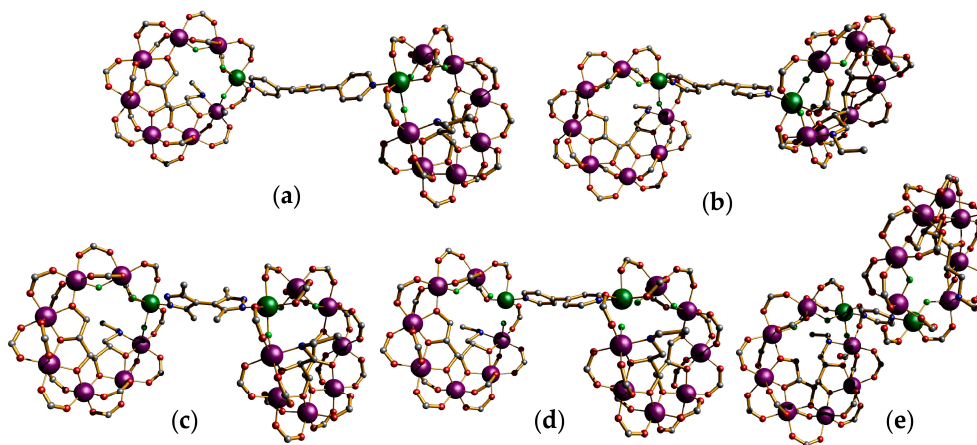


Figure 2. Crystal structures of the dimeric wheel assemblies $\{Cr_7Ni\}'_2L$, with L = bpbz (a); bpe (b); bpz (c); 4,4'-bpy (d); and pyr (e) (adapted from References [43–45]). Colour code: Cr, purple; Ni, green; N, blue; O, red; C, grey; F, pale green. H atoms and tertiary butyl groups are omitted for clarity.

The use of aromatic bridging ligands of varying length acting as additional bridging ligands between the Ni^{II} ions along this $\{Cr_7Ni\}'_2L$ series (L = pyr, 4,4'-bpy, and bpe) allows for the tunable variation of the electron exchange (EE) interaction between the two $\{Cr_7Ni\}'$ wheels separated by inter-ring intermetallic distances in the range of 7.0–15.4 Å, as confirmed by very low-temperature micro-SQUID magnetisation measurements. Therefore, an overall downward field shift of the inflection points (H_c) in the isothermal magnetisation curves at 0.04 K occurs along this series of dimers following the trend 30 (pyr) > 5 (4,4'-bpy) > 4 kOe (bpe), thus reflecting the weakening of the intramolecular magnetic coupling constant [$-J$ = 1.4 (pyr), 0.22 (4,4'-bpy), and 0.18 cm^{-1} (bpe)]. In fact, the gap between inflection points in the magnetization curves is directly related to the energy gap between the ground singlet ($S = 0$) and excited triplet ($S = 1$) pair states of the dimer [$\Delta E_{ST} = E(S = 0) - E(S = 1) = J$] [43–45]. Yet, these inter-ring magnetic interactions across the aromatic bridging ligands within the ring dimers would give rise to gate times that are shorter than the manipulation time of a single qubit, thus precluding their examination as candidates for a quantum gate through pulsed EPR experiments.

In order to decrease the EE interaction between $\{Cr_7Ni\}'$ wheels, Ardavan et al. have prepared a related series of wheel dimers of general formula $[\{Cr_7NiF_3(piv)_{15}(etglu)\}_2L_n]$, abbreviated as $\{Cr_7Ni\}'_2L_n$, with longer polypyridine bridging ligands functionalised with one (L_1 and L_2) or two (L_3) low-spin iron(II)-tris(dioximato) complexes of boronic acid-capped clathrochelate-type as central diamagnetic linkers, as depicted in Figure 3. Within this series of wheel dimers, they could tune the $Ni \cdots Ni$ distance from 18.9 (L_1) to 27.1 Å (L_2) and up to 30.7 Å (L_3). These $\{Cr_7Ni\}'_2L_n$ wheel dimers do not show evidence of coupling by continuous wave-EPR, so in order to characterise such a small EE interaction a pulsed-EPR technique called double electron–electron resonance (DEER) was used. For the longest linker (L_3) the two-qubit time of 550 ns is too long, as all these individual $\{Cr_7Ni\}'$ wheels showed T_M values around 600 ns at 2.5 K. In contrast, the shorter version (L_1) shows a slow gate time of 157 ns, which makes this compound suitable to implement a two-qubit conditional phase gate [41].

Thus, these examples exemplify how through supramolecular chemistry it is possible to tune, with control, the EE interaction between qubits and the two-qubit gate time. These are remarkable features that have not yet been achieved with other approaches of quantum computing.

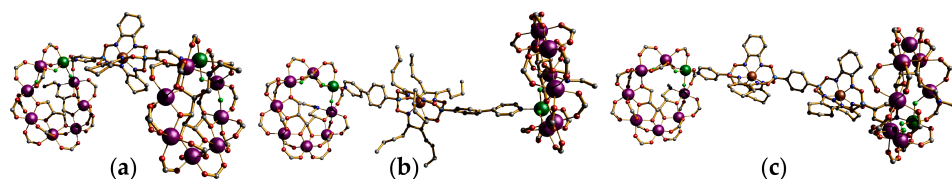


Figure 3. Crystal structures of the dimeric wheel assemblies $\{Cr_7Ni\}'_2L_n$ featuring mono- and dinuclear iron(II)-tris(dioximato) complexes of boronic acid-capped clathrochelate-type polypyridine ligands as central linkers, with $n = 1$ (a); 2 (b); and 3 (c) (adapted from Reference [45]). Colour code: Cr, purple; Ni, green; N, blue; O, red; C, grey; F, pale green. H atoms and tertiary butyl groups are omitted for clarity.

3.2. $\{Cr_7Ni\}$ Wheels as Metalloligands

The second route implies the functionalisation of the $\{Cr_7Ni\}$ wheels at the carboxylate ligand, which allow them to act as metalloligands towards other metal ions or complexes. Carboxylate substitution has proven to be a well-established chemical approach to achieve a selective functionalisation of $\{Cr_7Ni\}$ wheels and other polynuclear clusters [46–48]. The key feature of $\{Cr_7Ni\}$ wheels is the presence of labile nickel(II) and kinetically inert chromium(III) ions. Then, any substitution reaction on the carboxylates would take place on the $Cr \cdots Ni$ edges, and not on the $Cr \cdots Cr$ ones. Also, it is worthy to note their chemical stability and remarkable solubility in non-polar solvents, which simplify the purification of the resultant products by column chromatography.

The most studied carboxylate substitution reaction has been the selective functionalisation of $\{Cr_7Ni\}$ wheels with *iso*-nicotinate (O_2C-py) [46,49–51]. The reaction of *iso*-nicotinic acid with $\{Cr_7Ni\}$ wheels in *n*-propanol yields a mixture of wheels of formula $(Pr_2NH_2)_2[\{Cr_7NiF_8(piv)_{16-x}(O_2C-py)_x\}]$, abbreviated as $\{Cr_7Ni-(O_2C-py)_x\}$, where $x = 0–4$. In a second step the different substituted wheels could be separated by column chromatography. The best performance takes place for the monosubstituted compound, which could be obtained on the multi-gram scale with the *iso*-nicotinate perpendicular to the main plane of the wheel.

The reaction of $\{Cr_7Ni-(O_2C-py)\}$ as a metalloligand towards $Cu(NO_3)_2$ or $[Cu_2(O_2C^tBu)_4(HO_2C^tBu)_2]$ generates the first two examples of wheel dimers of the general formula $(Pr_2NH_2)_2[\{Cr_7NiF_8(piv)_{15}(O_2C-py)_2M\}]$ [$M = Cu(NO_3)_2(H_2O)$ and $Cu_2(O_2C^tBu)_4$], in short $\{Cr_7Ni\}_2Cu$ and $\{Cr_7Ni\}_2Cu_2$, respectively. In this work, Timco et al. experimentally demonstrated that it is possible to control the coupling in molecular spin clusters [46]. In particular, when mononuclear copper(II) is the central node, they observed the EPR spectrum of three weakly interacting $S = 1/2$ centers. Conversely, when the linker is the paddle-wheel dicopper(II) pivalate, where the strong antiferromagnetic interaction between copper centers gives rise to a diamagnetic node, the EPR spectrum of a single wheel is observed.

Chiesa et al. have extended this concept and reported a series of wheel dimers of the general formula $(Pr_2NH_2)_2[\{Cr_7NiF_8(piv)_{15}L\}_2NiL']_2$ [$L = iso$ -nicotinate (O_2C-py) and pyridazine-4-carboxylate ($O_2C-pydca$); $L' =$ acetylacetonate (*acac*), 1,1,1-trifluoroacetylacetonate (*tfacac*), and 1,1,1,5,5,5-hexafluoroacetylacetonate (*hfacac*)], abbreviated as $\{Cr_7NiL\}_2NiL'_2$, and depicted in Figure 4 [50]. In this case, the synthetic strategy is based on the use of $\{Cr_7Ni\}$ wheels with pyridine or pyridazine-functionalized carboxylate bridging ligands (*L*) which are able to further coordinate in either *cis* or *trans* disposition to coordinatively unsaturated nickel(II) complexes with two acetylacetonate or their fluoro-derivatives as blocking ligands (*L'*), to afford the resulting ring dimers with orthogonal or linear dispositions, respectively. The authors argued that the anisotropic nature of the mononuclear nickel(II) complex acting as the central linker along this $\{Cr_7NiL\}_2NiL'_2$ series may serve as a promising candidate for the switching of the electronic interaction in an entangled double qubit-based QG. Therefore, the effective magnetic coupling between the peripheral $S = 1/2$ $\{Cr_7Ni\}$ wheels and

the central $S = 1$ Ni^{II} complex is given by $J_{\text{eff}} = 1.13 J_{\text{CrNi}} - 0.63 J_{\text{NiNi}}$ ($|J_{\text{eff}}| = 0.004\text{--}0.221 \text{ cm}^{-1}$). The feasibility of these QGs precisely rely on the weakness of this intramolecular EE interaction with respect to the local magnetic anisotropy of the central linker ($D_{\text{Ni}} = 2.18\text{--}5.81 \text{ cm}^{-1}$).

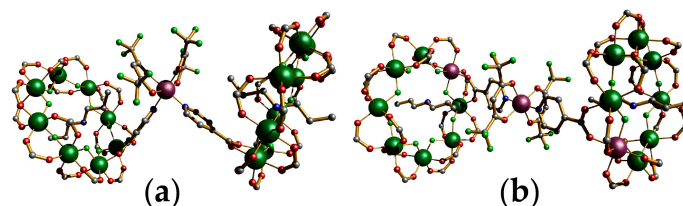


Figure 4. Crystal structures of the *cis*- (a) and *trans*- (b) dimeric wheel assemblies $\{\text{Cr}_7\text{NiL}\}_2\text{NiL}'_2$, with $L = \text{O}_2\text{C-py}$ and $L' = \text{hfac}$ (adapted from Reference [50]). Colour code: Cr, green; Ni, purple; N, blue; O, red; C, grey; F, pale green. H atoms and tertiary butyl groups are omitted for clarity.

More recently, Ferrando-Soria et al. have definitely demonstrated the validity of this supramolecular chemical approach for the physical implementation of double qubits-based QGs [52]. They have reported the assembly of a related pair of hetero- and homoleptic wheel dimers of formula $(\text{Pr}_2\text{NH}_2)_2\{[\text{Cr}_7\text{NiF}_8(\text{piv})_{15}L]\{[\text{Cr}_7\text{NiF}_8(\text{piv})_{15}L']\}\text{Co}(\text{NCS})_2\}$ [$L = \textit{iso}$ -nicotinate ($\text{O}_2\text{C-py}$) and $L' = 4$ -carboxylate-2,2':6':2''-terpyridine ($\text{O}_2\text{C-terpy}$)] and $(\text{Pr}_2\text{NH}_2)_2\{[\text{Cr}_7\text{NiF}_8(\text{piv})_{15}L']\}_2\text{Co}(\text{BF}_4)_2$ [$L'' = 4$ -carboxylate-2,2':6':2''-terpyridine ($\text{O}_2\text{C-terpy}$) or 4'-(4-phenylcarboxylate)-2,2':6':2''-terpyridine ($\text{O}_2\text{C-Ph-terpy}$)], abbreviated as $\{\text{Cr}_7\text{Ni}(L/L')\}_2\text{Co}$ and $\{\text{Cr}_7\text{Ni}L''\}_2\text{Co}$, respectively, from the use of $(\text{Pr}_2\text{NH}_2)\{[\text{Cr}_7\text{NiF}_8(\text{piv})_{15}L]\}$, $(\text{Pr}_2\text{NH}_2)\{[\text{Cr}_7\text{NiF}_8(\text{piv})_{15}L']\}$, and/or $(\text{Pr}_2\text{NH}_2)\{[\text{Cr}_7\text{NiF}_8(\text{piv})_{15}L'']\}$ wheels as metalloligands toward cobalt(II) ions, as illustrated in Figure 5.

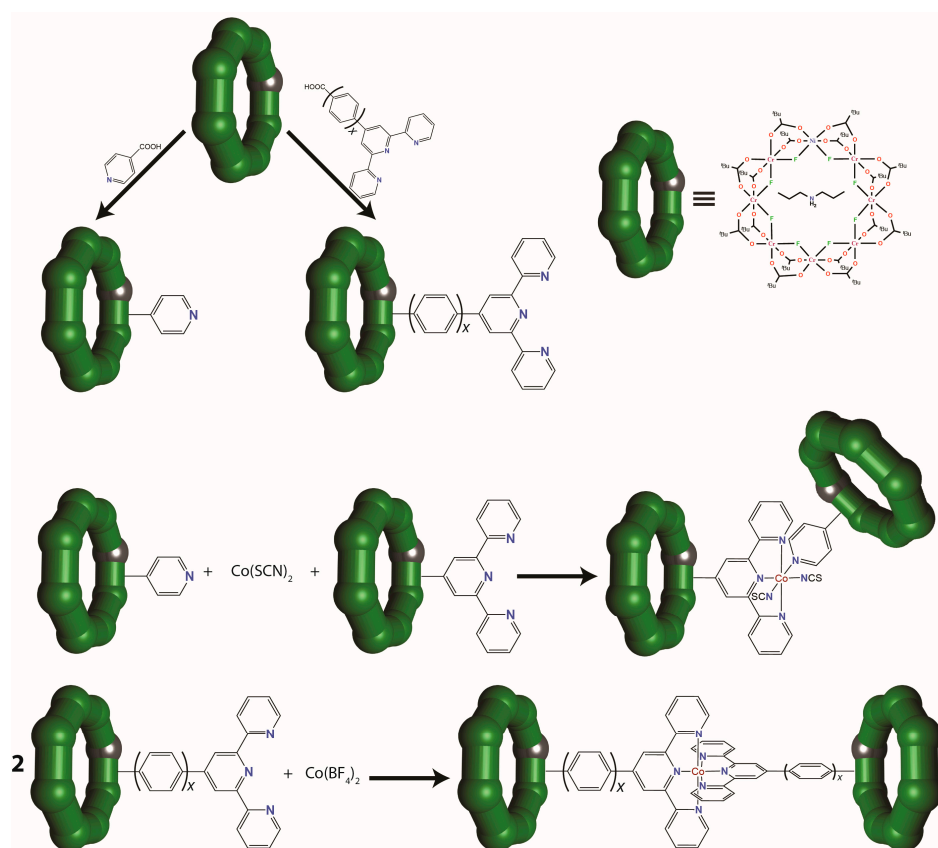


Figure 5. Supramolecular design strategy for the construction of two-qubit assemblies based on $\{\text{Cr}_7\text{Ni}\}$ wheels as individual molecular qubits (adapted from Reference [52]).

Depending on the choice of the central linker, these $\{\text{Cr}_7\text{Ni}(L/L')\}_2\text{Co}$ and $\{\text{Cr}_7\text{Ni}L''\}_2\text{Co}$ assemblies would operate as either controlled NOT-gate (CNOT) ($L = \text{O}_2\text{C-py}$ and $L' = \text{O}_2\text{C-terpy}$) or \sqrt{i} SWAP ($L'' = \text{O}_2\text{C-terpy}$ or $\text{O}_2\text{C-Ph-terpy}$) molecular logic gates for QIP, respectively, as depicted in Figure 6. The effect of the CNOT and \sqrt{i} SWAP gate on the computational two-qubit basis are [52]:

$$\begin{aligned} \text{CNOT: } & |00\rangle \rightarrow |00\rangle; |01\rangle \rightarrow |01\rangle; |10\rangle \rightarrow |11\rangle; |11\rangle \rightarrow |10\rangle \\ \sqrt{i}\text{SWAP: } & |00\rangle \rightarrow |00\rangle; |01\rangle \rightarrow \frac{|01\rangle + i|10\rangle}{\sqrt{2}}; |10\rangle \rightarrow \frac{|10\rangle + i|01\rangle}{\sqrt{2}}; |11\rangle \rightarrow |11\rangle \end{aligned}$$

Hence, for a QG initialised in the computational basis states $|11\rangle$ and $|10\rangle$, the CNOT flips the target qubit if the control is set to $|1\rangle$; this implies that the two qubits have to respond unequally to an external stimulus. Whereas for a QG initialised in the computational basis state $|10\rangle$, the \sqrt{i} SWAP brings it to the equal-weight superposition $(|10\rangle + i|01\rangle)/\sqrt{2}$ as soon as the inter-qubit interaction is turned on; this requires an electro-switchable linker between identical qubits. When cobalt(II) thiocyanate is used, the *cis* coordination of thiocyanate groups means that the linked $\{\text{Cr}_7\text{Ni}(\text{O}_2\text{C-py})\}$ and $\{\text{Cr}_7\text{Ni}(\text{O}_2\text{C-terpy})\}$ qubits are arranged in an almost orthogonal orientation. Therefore, the two qubits are symmetry inequivalent, as required for implementing a CNOT gate. Instead, with cobalt(II) tetrafluoroborate the assembly is made up of two equivalent $\{\text{Cr}_7\text{Ni}(\text{O}_2\text{C-terpy})\}$ or $\{\text{Cr}_7\text{Ni}(\text{O}_2\text{C-Ph-terpy})\}$ qubits separated by a redox-switchable centre, which makes these assemblies the first reported examples that are suitable for the implementation of the \sqrt{i} SWAP gate [52].

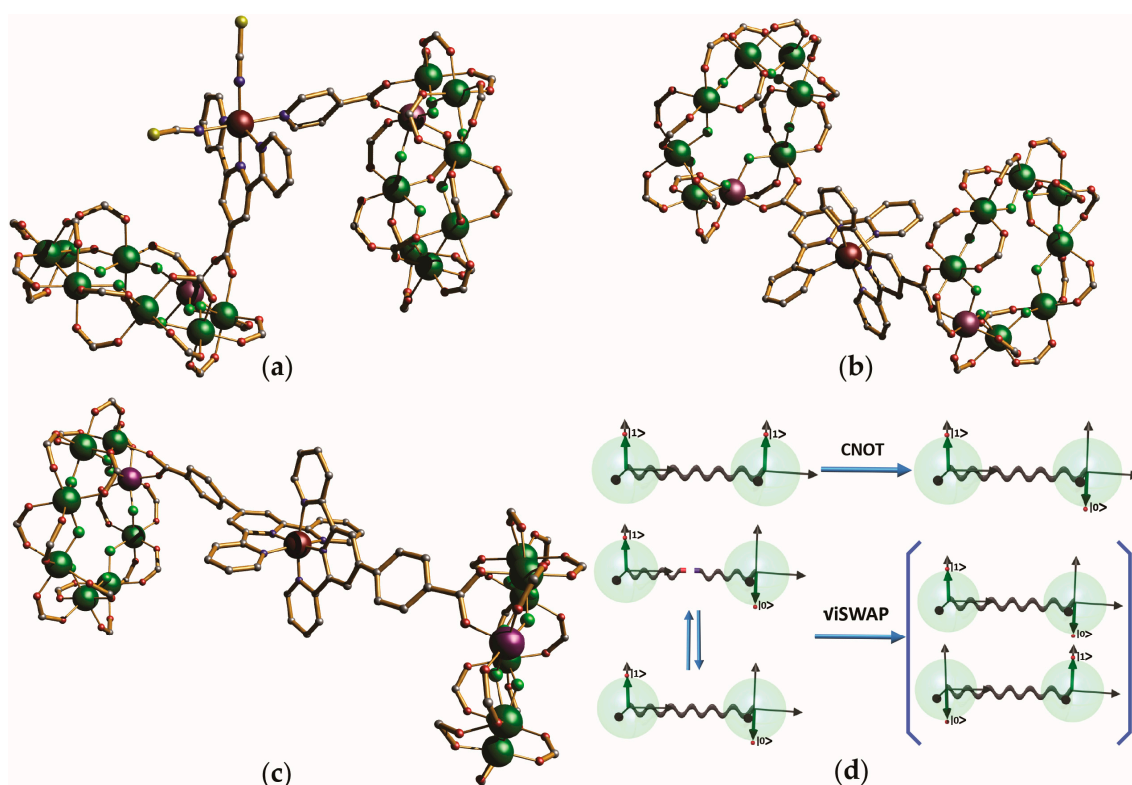


Figure 6. Crystal structures of the dimeric wheels assemblies $\{\text{Cr}_7\text{Ni}(L/L')\}_2\text{Co}$ and $\{\text{Cr}_7\text{Ni}L''\}_2\text{Co}$, with $L = \text{O}_2\text{C-py}$ and $L' = \text{O}_2\text{C-terpy}$ (a); $L'' = \text{O}_2\text{C-terpy}$ (b) or $\text{O}_2\text{C-Ph-terpy}$ (c). Colour code: Cr, green; Ni, purple; N, blue; O, red; C, grey; F, pale green. H atoms and tertiary butyl groups are omitted for clarity. (d) Schematic representation of the operational mode of the CNOT (controlled NOT-gate) and \sqrt{i} SWAP gates on a pair of qubits (adapted from Reference [52]).

3.3. $[\text{Cr}_7\text{Ni}]$ Wheels as Inorganic Macrocyclic Subunits of Hybrid Rotaxanes

The requirement of ammonium cations that template the formation of $[\text{Cr}_7\text{Ni}]$ wheels have also been exploited by Winpenny's group to create hybrid inorganic-organic rotaxanes [53–57]. They have

shown that it is possible to obtain in high yields [2]- and [3]-rotaxanes from the reaction in pivalic acid of chromium(III) trifluoride, a nickel(II) pivalate salt, and a thread with one or two amines, respectively, that would be protonated during the reaction and then act as template cations. Once again, the beauty and simplicity of this approach has allowed them to achieve great control at the supramolecular level that can yield a vast number of possibilities to construct different derivatives by changing the nature of the thread, through simple organic chemistry or by changing the carboxylate bridging ligand used to form the wheels.

Implementing two-qubits gates using hybrid rotaxanes has been done using two different approaches (Figure 7). The first one involves directly growing [3]-rotaxanes, whereby variation of the distance between the amine groups that template the formation of the wheels, it is possible to control the interaction between the qubits. Ardavan et al. have demonstrated this concept for a related series of [3]-rotaxanes proposed as candidates for entangled double qubit-based QGs ($T_M = 0.80\text{--}3.24 \mu\text{s}$ at 2.5 K) [45], whereby the through space inter-ring magnetic interaction between the two Cr_7Ni wheels is expected to be purely dipolar and modulated by the length of the thread. The second approach involves growing [2]- or [3]-rotaxanes where one or both ends of the thread are functionalised with a pyridine group as a stopper. Fernandez et al. have exploited this pathway through the reaction of the [2]- and [3]-rotaxanes of formula $[\text{PyCH}_2\text{NH}_2\text{CH}_2\text{CH}_2\text{Ph}][\text{Cr}_7\text{Ni}(\mu\text{-F})_8(\text{O}_2\text{C}^t\text{Bu})_{16}]$ and $\{\text{PyCH}_2\text{NH}_2(\text{CH}_2)_5\}_2[\text{Cr}_7\text{Ni}(\mu\text{-F})_8(\text{O}_2\text{C}^t\text{Bu})_{16}]_2$, in short $\{\text{Cr}_7\text{Ni-Py}\}$ and $\{\text{Py-(Cr}_7\text{Ni)}_2\text{-Py}\}$, respectively, with copper(II) hexafluoroacetylacetonate, $[\text{Cu}(\text{hfacac})_2]$, to obtain the resulting $\{\text{Cr}_7\text{Ni-Py}\}[\text{Cu}(\text{hfacac})_2]$ and $\{\text{Py-(Cr}_7\text{Ni)}_2\text{-Py}\}[\text{Cu}(\text{hfacac})_2]_2$ derivatives [56]. These new organic-inorganic [2]- and [3]-rotaxanes should not present interactions between the copper(II) centers and the wheels, acting as dissimilar qubits, because the only through-bond EE interaction involves hydrogen bonds. However, in both cases, a weak antiferromagnetic interaction is observed by EPR spectroscopy between the wheels and the copper(II) ions. In addition, the different g factors of the qubits that are brought together open the possibility of addressing each qubit individually, in the so called g -engineering approach. Thus, the heterospin nature of $\{\text{Cr}_7\text{Ni-Py}\}[\text{Cu}(\text{hfacac})_2]$ together with the weak EE interaction make this assembly a suitable candidate to implement the CNOT gate. More interesting is the feasible scalability of such physical behavior by applying basic concepts in chemistry, as it is well performed with $\{\text{Py-(Cr}_7\text{Ni)}_2\text{-Py}\}[\text{Cu}(\text{hfacac})_2]_2$.

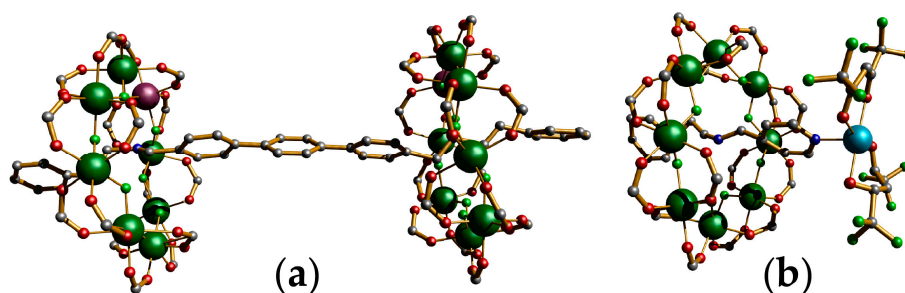


Figure 7. Crystal structures of a [3]-rotaxane (a) and a [2]-rotaxane (b) that show the two approaches that could be followed with hybrid rotaxanes to build two-qubit gates (adapted from References [44,55]). Colour code: Cr, green; Ni, purple; Cu, light blue; N, blue; O, red; C, grey; F, pale green. H atoms and tertiary butyl groups are omitted for clarity.

4. Oligomeric Arrays of $\{\text{Cr}_7\text{Ni}\}$ Wheels as Multiple Qubits

Winpenny's group keeps spinning the wheel by using supramolecular chemistry methods to obtain new families of nanosized oligomeric wheel derivatives. Different shapes (planar or globular) and degrees of polymerisation, from dimers to trimers, tetramers, hexamers, or even larger oligomers with different polymerisation degrees ($P = 2, 3, 4, 6,$ and 24). As well as, a variety of potentially switchable, diamagnetic and paramagnetic linkers of either organic or metalloorganic nature.

So, for instance, Fernandez et al. have recently prepared a unique series of linear and branched, hybrid organic-inorganic polyrotaxanes, referred to as $[n]$ -rotaxanes ($n = 3-7$), whereby the functionalised organic thread component templates the hydrogen bond-assisted self-assembly of the inorganic $\{Cr_7Ni\}$ wheels about the organic axle. The larger [3]-, [4]-, [5]-, and [7]-rotaxanes are built up from simpler [2]- and [3]-rotaxanes and diverse central linkers such as mononuclear copper(II) complexes, $[Cu(NO_3)_2]$ and $[Cu(hfacac)_2]$, paddle-wheel dicopper(II) complexes, $[Cu_2(piv)_4]$, and oxo-centered iron(III)-cobalt(II) triangles, $[Fe_2CoO(piv)_6]$, as illustrated in Figure 8 [57]. Interestingly, these $[n]$ -rotaxanes exhibited T_M values in the range of 0.70 to 0.80 μ s at 2.6 K, and in some of them, two-qubit interactions of the right strength to implement logic quantum gates have been found. This work nicely exemplifies how through the application of basic concepts such as coordination and supramolecular chemistry we can create a supramolecular array of molecular qubits, where the individual qubits retain their coherence time, and the strength of inter-qubit interaction could be modulated by chemical design.

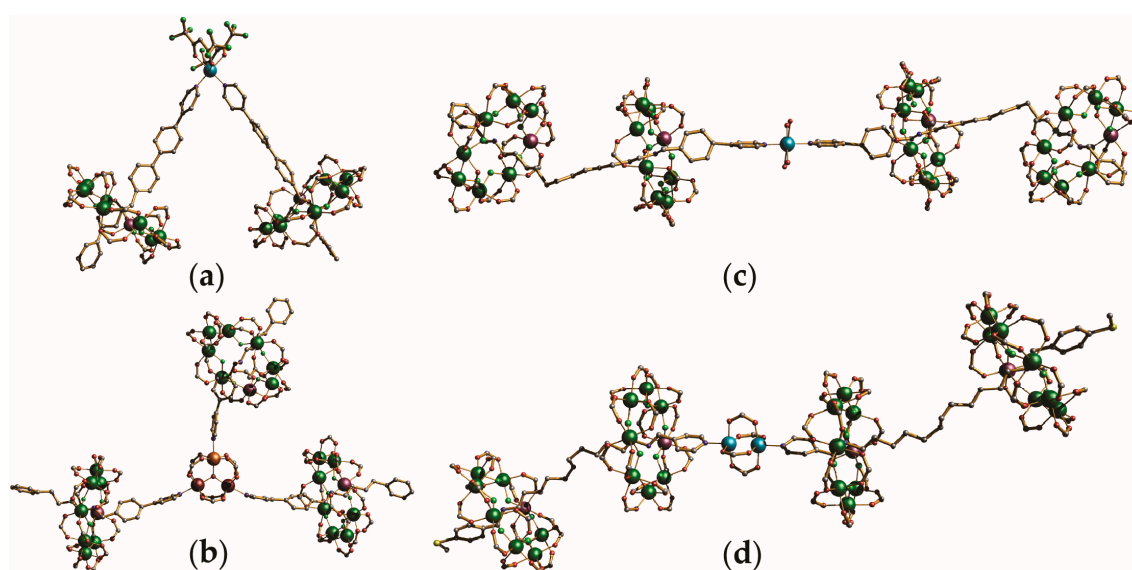


Figure 8. Crystal structures of linear and branched [3]- (a); [4]- (b); and [5]-rotaxane-type (c,d), oligomeric $\{Cr_7Ni\}$ wheel assemblies (adapted from Reference [57]). Colour code: Cr, green; Fe, brown; Co, orange; Ni, purple; Cu, light blue; N, blue; O, red; C, grey; F, pale green. H atoms and tertiary butyl groups are omitted for clarity.

Alternatively, Whitehead et al. obtained a plethora of metalloorganic-inorganic multicomponent supramolecular assemblies, such as metal polygons and polyhedra, using pyridine- or carboxylate-functionalised $\{Cr_7Ni\}$ wheels as metalloligands. They are constructed from hydroxo-bridged copper(II) squares, $[Cu_4(OH)_4]$, oxo-centered iron(III)-cobalt(II) triangles or zinc(II) tetrahedra, $[Fe_2CoO]$ or $[Zn_4O]$, oxo-centered edge-sharing manganese(II,III) tetrahedra, $[Mn_6O_2]$, and nickel(II) dodecagons, $[Ni_{12}]$, as central linkers surrounded by Cr_7Ni wheels, as illustrated in Figure 9 [49,58]. In each case, the interactions between the Cr_7Ni wheels and the diverse metal coordination cages of these multicomponent assemblies are very weak, as shown by their variable-temperature magnetic susceptibility and variable-field magnetisation measurements. Their total magnetic behaviour is the sum of those of their individual components, even if their quantum coherence properties have not yet been measured through pulsed EPR measurements.

Following this same modular design strategy, Ferrando-Soria et al. have recently prepared a nanoscopic metal coordination cage formed by the palladium(II)-mediated self-assembly of up to 24 Cr_7Ni wheels, as illustrated in Figure 10 [59]. Remarkably, pulsed EPR measurements reveal that the quantum coherence of the individual Cr_7Ni wheel component is almost retained in the resulting

nanocage assembly, with T_M values of 0.41 and 0.35 μ s at 5.0 K for isolated and assembled wheels, respectively, thus paving the way to obtain QGs based on very large arrays of qubits.

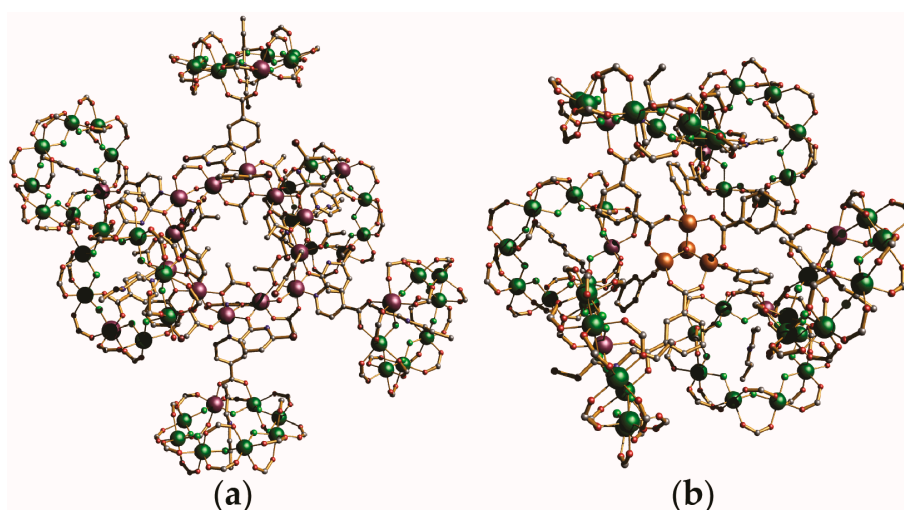


Figure 9. Crystal structures of pyridine- (a) and carboxylate-functionalised (b), oligomeric $\{Cr_7Ni\}$ wheel assemblies (adapted from References [49,58]). Colour code: Cr, green; Ni, purple; Zn, orange; N, blue; O, red; C, grey; F, pale green. H atoms and tertiary butyl groups are omitted for clarity.

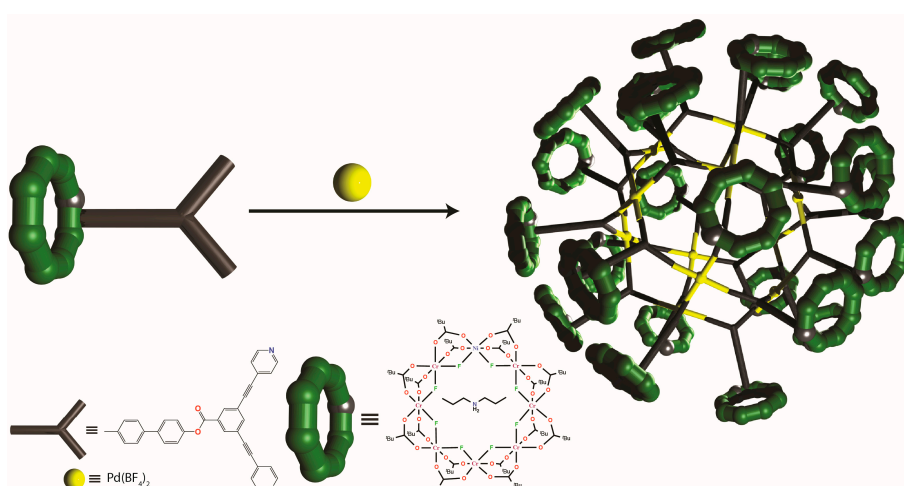


Figure 10. Supramolecular design strategy for the construction of multiple-qubit arrays based on $\{Cr_7Ni\}$ wheels as individual molecular qubits (adapted from Reference [59]).

5. Conclusions and Perspectives

In this review, we have tried to exemplify how supramolecular chemistry approaches could have a major impact on the physical implementation of QIP. This has been exemplified through the latest results obtained by Winpenney's group in Manchester, UK, using $\{Cr_7Ni\}$ wheels as a proof-of-concept design for molecular qubits. In fact, the high degree of chemical versatility, at both the molecular and supramolecular levels, makes these systems suitable candidates to prove the validity and applicability of molecules for quantum computation applications. However, the construction of molecule-based quantum computers would require more long-lived qubits that can perform much more logic operations without errors. Electron spins possess shorter relaxation and coherence times than nuclear spins due to their stronger coupling with the environment; however, it is precisely because of this that they are easier to address and manipulate, and consequently, more prone to use as active components of quantum computers.

Recent studies by van Slageren and Sessoli's groups [60,61] have ascertained that the origin of the larger T_M values (even at 300 K) observed for mononuclear V(IV) [21,22] and Cu(II) [16,18] complexes over those of {Cr₇Ni} wheels is likely related to the coordination geometry and small spin-orbit coupling of the single metal ions in the former case, as well as the minimal contact of the magnetic orbital with the surrounding matrix, and the rigidity of the molecular structure. On the other hand, for the {Cr₇Ni} wheels it has been found that the main source of decoherence is related to the electron-nuclear spin (hyperfine) coupling. However, the relationship between the intra-wheel exchange interactions and the T_M is not obvious. In principle, hyperfine and dipolar interactions should not be influenced by a change of the intra-ring exchange couplings. Conversely, spin-phonon interaction may be influenced by it.

Thus, it is obvious that magnetic molecules are strong candidates for the implementation of logic schemes in QIP. The next step for all the proposed qubits would be to implement QGs by following the routes that {Cr₇Ni} wheels opened several years ago in order to construct assemblies of entangled qubits, without losing their individual quantum coherence properties. This will probably not be an easy task, because it is not a trivial problem and each molecule would require a particular approach. However, while trying to achieve these targets, new and exciting physical properties can be discovered, which can also enrich the background of the molecule-based materials community.

Acknowledgments: This work was supported by the MINECO (Spain) (Projects CTQ2013-46362-P, CTQ2013-44844-P, and Excellence Unit "Maria de Maeztu" MDM-2015-0538). Thanks are also extended to the "Convocatoria 2015 de Ayudas Fundación BBVA a Investigadores y Creadores Culturales" for a postdoctoral contract. J.F.-S. is especially thankful to Richard Winpenny for his stimulating supervision during his postdoctoral stay at the Manchester Molecular Magnetism Group and the opportunity given to write this review. J.F.-S. would also like to extend thanks to the rest of the group, and especially to Eric McInnes, David Collison, and Floriana Tuna, Grigore Timco, Antonio Fernandez, as well as to Christopher Muryn and Iñigo Vitorica (University of Manchester), and Stefano Carretta and Paolo Santini and Alessandro Chiesa (Università de Parma), for their continuous advice, help, and collaborative work. J.F.-S. is also thankful to Emilio Pardo and Rafael Ruiz Garcia (ICMol, Universitat de València) for their supporting help and fruitful discussions during the realisation of this review.

Conflicts of Interest: The author declares no conflict of interest.

References

1. Feynman, R.P. Simulating physics with computers. *Int. J. Theor. Phys.* **1982**, *21*, 467–488. [[CrossRef](#)]
2. Lloyd, S. Universal quantum simulators. *Science* **1996**, *273*, 1073–1078. [[CrossRef](#)] [[PubMed](#)]
3. Nielsen, M.A.; Chuang, I.L. *Quantum Computation and Quantum Information*; Cambridge University Press: New York, NY, USA, 2000.
4. Ladd, T.D.; Jelezko, F.; Laflamme, R.; Nakamura, Y.; Monroe, C.; O'Brien, J.L. Quantum computers. *Nature* **2010**, *464*, 45–53. [[CrossRef](#)] [[PubMed](#)]
5. Shor, P.W. Polynomial-time algorithms for prime factorization and discrete logarithms on a quantum computer. *SIAM J. Comput.* **1997**, *26*, 1484–1509. [[CrossRef](#)]
6. Grover, L.K. Quantum computers can search arbitrarily large databases by a single query. *Phys. Rev. Lett.* **1997**, *79*, 4709–4712. [[CrossRef](#)]
7. Leuenberger, M.; Loss, D. Simulating physics with computers. *Nature* **2001**, *410*, 789–793. [[CrossRef](#)] [[PubMed](#)]
8. Meier, F.; Levy, J.; Loss, D. Quantum computing with spin cluster qubits. *Phys. Rev. Lett.* **2003**, *90*, 47901–47904. [[CrossRef](#)] [[PubMed](#)]
9. Troiani, F.; Affronte, M.; Carretta, S.; Santini, P.; Amoretti, G. Proposal for quantum gates in permanently coupled antiferromagnetic spin rings without need of local fields. *Phys. Rev. Lett.* **2005**, *94*, 190501. [[CrossRef](#)] [[PubMed](#)]
10. Lehmann, J.; Gaita-Ariño, A.; Coronado, E.; Loss, D. Spin qubits with electrically gated polyoxometalate molecules. *Nat. Nanotechnol.* **2007**, *2*, 312–317. [[CrossRef](#)] [[PubMed](#)]
11. Ardavan, A.; Rival, O.; Morton, J.J.L.; Blundell, S.J.; Tyryshkin, A.M.; Timco, G.A.; Winpenny, R.E.P. Will spin-relaxation times in molecular magnets permit quantum information processing? *Phys. Rev. Lett.* **2007**, *98*, 057201. [[CrossRef](#)] [[PubMed](#)]

12. Kitagawa, M.; Nakasuji, K.; Takui, T. Triple-stranded metallo-helicates addressable as Lloyd's electron spin qubits. *J. Am. Chem. Soc.* **2010**, *132*, 6944–6946.
13. Nakazawa, S.; Nishida, S.; Ise, T.; Yoshino, T.; Mori, N.R.; Rahimi, D.; Sato, K.; Morita, Y.; Toyota, K.; Shiomi, D.; et al. A synthetic two-spin quantum bit: *g*-engineered exchange-coupled biradical designed for controlled-NOT gate operations. *Angew. Chem. Int. Ed.* **2012**, *51*, 9860–9864. [[CrossRef](#)] [[PubMed](#)]
14. Wedge, C.J.; Timco, G.A.; Spielberg, E.T.; George, R.E.; Tuna, F.; Rigby, S.; McInnes, E.J.L.; Winpenny, R.E.P.; Blundell, S.J.; Ardavan, A. Chemical engineering of molecular qubits. *Phys. Rev. Lett.* **2012**, *108*, 107204. [[CrossRef](#)] [[PubMed](#)]
15. Aromí, G.; Aguilà, D.; Gamez, P.; Luis, F.; Roubeau, O. Design of magnetic coordination complexes for quantum computing. *Chem. Soc. Rev.* **2012**, *41*, 537–546.
16. Warner, M.; Din, S.; Tupitsyn, I.S.; Morley, G.W.; Stoneham, A.; Gardener, J.A.; Wu, Z.; Fisher, A.J.; Heutz, S.; Kay, C.W.M.; et al. Potential for spin-based information processing in a thin-film molecular semiconductor. *Nature* **2013**, *503*, 504–508. [[CrossRef](#)] [[PubMed](#)]
17. Graham, M.J.; Zadrozny, J.M.; Shiddiq, M.; Anderson, J.S.; Fataftah, M.S.; Hill, S.; Freedman, D.E. Influence of electronic spin and spin-orbit coupling on decoherence in mononuclear transition metal complexes. *J. Am. Chem. Soc.* **2014**, *136*, 7623–7626. [[CrossRef](#)] [[PubMed](#)]
18. Bader, K.; Dengler, D.; Lenz, S.; Endeward, B.; Jiang, S.D.; Neugebauer, P.; Slageren, J. Room temperature quantum coherence in a potential molecular qubit. *Nat. Commun.* **2014**, *5*, 5304. [[CrossRef](#)] [[PubMed](#)]
19. Aguilà, D.; Barrios, L.A.; Velasco, V.; Roubeau, O.; Repollés, A.; Alonso, P.J.; Sesé, J.; Teat, S.J.; Luis, F.; Aromí, G. Heterodimetallic [LnLn'] Lanthanide complexes: Toward a chemical design of two-qubit molecular spin quantum gates. *J. Am. Chem. Soc.* **2014**, *136*, 14215–14222. [[CrossRef](#)] [[PubMed](#)]
20. Walsh, J.P.S.; Meadows, S.B.; Ghirri, A.; Moro, F.; Jennings, M.; Smith, W.F.; Graham, D.M.; Kihara, T.; Nojiri, H.; Vitorica-Yrezabal, I.; et al. Electronic structure of a mixed-metal fluoride-centered triangle complex: A potential qubit component. *Inorg. Chem.* **2015**, *54*, 12019–12026. [[CrossRef](#)] [[PubMed](#)]
21. Zadrozny, J.M.; Niklas, J.; Poluektov, O.G.; Freedman, D.E. Millisecond coherence time in a tunable molecular electronic spin qubit. *ACS Cent. Sci.* **2015**, *1*, 488–492. [[CrossRef](#)] [[PubMed](#)]
22. Atzori, M.; Tesi, L.; Morra, E.; Chiesa, M.; Sorace, L.; Sessoli, R. Room-temperature quantum coherence and rabi oscillations in vanadyl phthalocyanine: Toward multifunctional molecular spin qubits. *J. Am. Chem. Soc.* **2016**, *138*, 2154–2157. [[CrossRef](#)] [[PubMed](#)]
23. Pedersen, K.S.; Ariciu, A.M.; McAdams, S.; Weihe, H.; Bendix, J.; Tuna, F.; Piligkos, S. Toward molecular 4f single-ion magnet qubits. *J. Am. Chem. Soc.* **2016**, *138*, 5801–5804. [[CrossRef](#)] [[PubMed](#)]
24. Shiddiq, M.; Komijani, D.; Duan, Y.; Gaita-Ariño, A.; Coronado, E.; Hill, S. Enhancing coherence in molecular spin qubits via atomic clock transitions. *Nature* **2016**, *531*, 348–351. [[CrossRef](#)] [[PubMed](#)]
25. Burkard, G.; Loss, D.; DiVincenzo, D.P. Coupled quantum dots as quantum gates. *Phys. Rev. B* **1999**, *59*, 2070–2078. [[CrossRef](#)]
26. Hanson, R.; Awschalom, D.D. Coherent manipulation of single spins in semiconductors. *Nature* **2008**, *453*, 1043–1049. [[CrossRef](#)] [[PubMed](#)]
27. Maurer, P.C.; Kucsko, G.; Latta, C.; Jiang, L.; Yao, N.Y.; Bennett, S.D.; Pastawski, F.; Hunger, D.; Chisholm, N.; Markham, M.; et al. Room-temperature quantum bit memory exceeding one second. *Science* **2012**, *336*, 1283–1286. [[CrossRef](#)] [[PubMed](#)]
28. Knowles, H.S.; Kara, D.M.; Atatüre, M. Observing bulk diamond spin coherence in high-purity nanodiamonds. *Nat. Mater.* **2014**, *13*, 21–25. [[CrossRef](#)] [[PubMed](#)]
29. Georgescu, I.M.; Ashhab, S.; Nori, F. Quantum simulation. *Rev. Mod. Phys.* **2014**, *86*, 153–185. [[CrossRef](#)]
30. Lehn, J.M. *Supramolecular Chemistry: Concepts and Perspectives*; Wiley-VCH: Weinheim, Germany, 1995.
31. Fujita, M.; Tominaga, M.; Hori, A.; Therrien, B. Coordination assemblies from a Pd(II)-cornered square complex. *Acc. Chem. Res.* **2005**, *38*, 371–380. [[CrossRef](#)] [[PubMed](#)]
32. Pluth, M.D.; Bergman, R.G.; Raymond, K.N. Supermolecules by design. *Acc. Chem. Res.* **2009**, *42*, 1650–1659. [[CrossRef](#)] [[PubMed](#)]
33. Chakrabarty, R.; Mukherjee, P.S.; Stang, P.J. Supramolecular coordination: Self-assembly of finite two- and three-dimensional ensembles. *Chem. Rev.* **2011**, *111*, 6810–6918. [[CrossRef](#)] [[PubMed](#)]
34. Ward, M.D.; Raithby, P.R. Functional behaviour from controlled self-assembly: Challenges and prospects. *Chem. Soc. Rev.* **2013**, *42*, 1619–1636. [[CrossRef](#)] [[PubMed](#)]

35. Schweiger, A.; Jeschke, G. *Principles of Pulse Electron Paramagnetic Resonance*; Oxford University Press: New York, NY, USA, 2001.
36. Affronte, M.; Carretta, S.; Timco, G.A.; Winpenny, R.E.P. A ring cycle: Studies of heterometallic wheels. *Chem. Commun.* **2007**, 1789–1797. [[CrossRef](#)] [[PubMed](#)]
37. Timco, G.A.; Faust, T.B.; Tuna, F.; Winpenny, R.E.P. Linking heterometallic rings for quantum information processing and amusement. *Chem. Soc. Rev.* **2011**, *40*, 3067–3075. [[CrossRef](#)] [[PubMed](#)]
38. McInnes, E.J.L.; Timco, G.A.; Whitehead, G.F.S.; Winpenny, R.E.P. Heterometallic rings: Their physics and use as supramolecular building blocks. *Angew. Chem. Int. Ed.* **2015**, *54*, 14244–14269. [[CrossRef](#)] [[PubMed](#)]
39. Candini, A.; Lorusso, G.; Troiani, F.; Ghirri, A.; Carretta, S.; Santini, P.; Amoretti, G.; Muryn, C.; Tuna, F.; Timco, G.; et al. Entanglement in supramolecular spin systems of two weakly coupled antiferromagnetic rings (Purple-Cr₇Ni). *Phys. Rev. Lett.* **2010**, *104*, 037203. [[CrossRef](#)] [[PubMed](#)]
40. Kaminski, D.; Webber, A.L.; Wedge, C.J.; Liu, J.; Timco, G.A.; Vitorica-Yrezabal, I.J.; McInnes, E.J.L.; Winpenny, R.E.P.; Ardavan, A. Quantum spin coherence in halogen-modified Cr₇Ni molecular nanomagnets. *Phys. Rev. B* **2014**, *90*, 184419. [[CrossRef](#)]
41. Ardavan, A.; Bowen, A.; Fernandez, A.; Fielding, A.; Kaminski, D.; Moro, F.; Muryn, C.A.; Wise, M.D.; Ruggi, A.; McInnes, E.J.L.; et al. Engineering coherent interactions in molecular nanomagnet dimers. *NPJ Quantum Inf.* **2015**, *1*, 15012. [[CrossRef](#)]
42. Timco, G.A.; McInnes, E.J.L.; Pritchard, R.G.; Tuna, F.; Winpenny, R.E.P. Heterometallic rings made from chromium stick together easily. *Angew. Chem. Int. Ed.* **2008**, *47*, 9681–9684. [[CrossRef](#)] [[PubMed](#)]
43. Faust, T.B.; Bellini, V.; Candini, A.; Carretta, S.; Lorusso, G.; Allan, D.R.; Carthy, L.; Collison, D.; Docherty, R.J.; Kenyon, J.; et al. Chemical control of spin propagation between heterometallic rings. *Chem. Eur. J.* **2011**, *17*, 14020–14030. [[CrossRef](#)] [[PubMed](#)]
44. Bellini, V.; Lorusso, G.; Candini, A.; Wernsdorfer, W.; Faust, T.B.; Timco, G.A.; Winpenny, R.E.P.; Affronte, M. Propagation of spin information at the supramolecular scale through heteroaromatic linkers. *Phys. Rev. Lett.* **2011**, *106*, 227205. [[CrossRef](#)] [[PubMed](#)]
45. Faust, T.B.; Tuna, F.; Timco, G.A.; Affronte, M.; Bellini, V.; Wernsdorfer, W.; Winpenny, R.E.P. Controlling magnetic communication through aromatic bridges by variation in torsion angle. *Dalton Trans.* **2012**, *41*, 13626–13631. [[CrossRef](#)] [[PubMed](#)]
46. Timco, G.A.; Carretta, S.; Troiani, F.; Tuna, F.; Pritchard, R.J.; Muryn, C.A.; McInnes, E.J.L.; Ghirri, A.; Candini, A.; Santini, P.; et al. Engineering the coupling between molecular spin qubits by coordination chemistry. *Nat. Nanotechnol.* **2008**, *4*, 173–178. [[CrossRef](#)] [[PubMed](#)]
47. Sessoli, R.; Tsai, H.L.; Schake, A.R.; Wang, S.; Vincent, J.B.; Folting, K.; Gatteschi, D.; Christou, G.; Hendrickson, D.N. High-spin molecules: [Mn₁₂O₁₂(O₂CR)₁₆(H₂O)₄]. *J. Am. Chem. Soc.* **1993**, *115*, 1804–1816. [[CrossRef](#)]
48. Soler, M.; Artus, P.; Folting, K.; Huffman, J.C.; Hendrickson, D.N.; Christou, G. Single-molecule magnets: Preparation and properties of mixed-carboxylate complexes [Mn₁₂O₁₂(O₂CR)₈(O₂CR')₈(H₂O)₄]. *Inorg. Chem.* **2001**, *40*, 4902–4912. [[CrossRef](#)] [[PubMed](#)]
49. Whitehead, G.F.S.; Moro, F.; Timco, G.A.; Wernsdorfer, W.; Teat, S.J.; Winpenny, R.E.P. A ring of rings and other multicomponent assemblies of cages. *Angew. Chem. Int. Ed.* **2013**, *52*, 9932–9935. [[CrossRef](#)] [[PubMed](#)]
50. Chiesa, A.; Whitehead, G.F.S.; Carretta, S.; Timco, G.A.; Carthy, L.; Teat, S.J.; Amoretti, G.; Pavarini, E.; Winpenny, R.E.P.; Santini, P. Molecular nanomagnets with switchable coupling for quantum simulation. *NPG Sci. Rep.* **2014**, *4*, 7423. [[CrossRef](#)] [[PubMed](#)]
51. Whitehead, G.F.S.; Ferrando-Soria, J.; Carthy, L.; Pritchard, R.G.; Teat, S.J.; Timco, G.A.; Winpenny, R.E.P. Synthesis and reactions of *N*-heterocycle functionalised variants of heterometallic {Cr₇Ni} rings. *Dalton Trans.* **2016**, *45*, 1638–1647. [[CrossRef](#)] [[PubMed](#)]
52. Ferrando-Soria, J.; Pineda, E.M.; Chiesa, A.; Fernandez, A.; Magee, S.A.; Carretta, S.; Santini, P.; Vitorica-Yrezabal, I.J.; Tuna, F.; Timco, G.A.; et al. A modular design of molecular qubits to implement universal quantum gates. *Nat. Commun.* **2016**, *7*, 11377. [[CrossRef](#)] [[PubMed](#)]
53. Lee, C.-F.; Leigh, D.A.; Pritchard, R.G.; Schultz, D.; Teat, S.J.; Timco, G.A.; Winpenny, R.E.P. Hybrid organic-inorganic rotaxanes and molecular shuttles. *Nature* **2009**, *458*, 314–318. [[CrossRef](#)] [[PubMed](#)]
54. Ballesteros, B.; Faust, T.B.; Lee, C.-F.; Leigh, D.A.; Muryn, C.A.; Pritchard, R.G.; Schultz, D.; Teat, S.J.; Timco, G.A.; Winpenny, R.E.P. Synthesis, structure and dynamic properties of hybrid organic-inorganic rotaxanes. *J. Am. Chem. Soc.* **2010**, *132*, 15435–15444. [[CrossRef](#)] [[PubMed](#)]

55. Whitehead, G.F.S.; Cross, B.; Carthy, L.; Milway, V.A.; Rath, H.; Fernandez, A.; Heath, S.L.; Muryn, C.A.; Pritchard, R.G.; Teat, S.J.; et al. Rings and threads as linkers in metal-organic frameworks and poly-rotaxanes. *Chem. Commun.* **2013**, *49*, 7195–7197. [[CrossRef](#)] [[PubMed](#)]
56. Fernandez, A.; Moreno Pineda, E.; Muryn, C.A.; Sproules, S.; Moro, F.; Timco, G.A.; McInnes, E.J.L.; Winpenny, R.E.P. *g*-Engineering in hybrid rotaxanes to create AB and AB₂ electron spin systems: EPR spectroscopic studies of weak interactions between dissimilar electron spin qubits. *Angew. Chem. Int. Ed.* **2015**, *54*, 10858–10861. [[CrossRef](#)] [[PubMed](#)]
57. Fernandez, A.; Ferrando-Soria, J.; Pineda, E.M.; Tuna, F.; Vitorica-Yrezabal, I.J.; Knappke, C.; Ujma, J.; Muryn, C.A.; Timco, G.A.; Barran, P.E.; et al. Making hybrid [*n*]-rotaxanes as supramolecular arrays of molecular electron spin qubits. *Nat. Commun.* **2016**, *7*, 10240. [[CrossRef](#)] [[PubMed](#)]
58. Whitehead, G.F.S.; Ferrando-Soria, J.; Christie, L.G.; Chilton, N.F.; Timco, G.A.; Moro, F.; Winpenny, R.E.P. The acid test: The chemistry of carboxylic acid functionalised {Cr₇Ni} rings. *Chem. Sci.* **2014**, *5*, 235–239. [[CrossRef](#)]
59. Ferrando-Soria, J.; Fernandez, A.; Pineda, E.M.; Varey, S.A.; Adams, R.W.; Vitorica-Yrezabal, I.J.; Tuna, F.; Timco, G.A.; Muryn, C.A.; Winpenny, R.E.P. Controlled synthesis of nanoscopic metal cages. *J. Am. Chem. Soc.* **2015**, *137*, 7644–7647. [[CrossRef](#)] [[PubMed](#)]
60. Bader, K.; Winkler, M.; van Slageren, J. Tuning of molecular qubits: Very long coherence and spin-lattice relaxation times. *Chem. Commun.* **2016**, *52*, 3623–3626. [[CrossRef](#)] [[PubMed](#)]
61. Atzori, M.; Morra, E.; Tesi, L.; Albino, A.; Chiesa, M.; Sorace, L.; Sessoli, R. Quantum coherence times enhancement in vanadium(IV)-based potential molecular qubits: The key role of the vanadyl moiety. *J. Am. Chem. Soc.* **2016**, *138*, 11234–11244. [[CrossRef](#)] [[PubMed](#)]



© 2016 by the author; licensee MDPI, Basel, Switzerland. This article is an open access article distributed under the terms and conditions of the Creative Commons Attribution (CC-BY) license (<http://creativecommons.org/licenses/by/4.0/>).